Fachtagung "Experimentelle Strömungsmechanik"
3. – 5. September 2019, Erlangen

Prevention or inhibition of foam formation through identification of non-existence domains in the interface in random and structured column-packings

Prävention oder Inhibierung der Schaumbildung durch Identifikation von Grenzflächen-Nichtexistenz-Domänen in Kolonnenfüllkörpern und –packungen

Lidia Almazan[1*], Anuhar Osorio-Nesme[1], Antonio Delgado[1]
[1] Lehrstuhl für Strömungsmechanik, Friedrich-Alexander-Universität Erlangen-Nürnberg, Cauerstr. 4, D-91058 Erlangen, Germany

Keywords: Foam, packings, column
Schlagworte: Schaum, Packungen, Kolonnen

Abstract

Undesired foams in reactors occupy the place 11 out of 31 of the causes of column malfunctions. These malfunctions are mainly caused by interfering with transport processes and chemical reactions up to the complete disruption of the process. The wide range of consequences (e.g. waste of time, energy, resources, costs …) affect the production of food as well as of fine chemicals. The influence of the shape of both random and structured packings on foam formation located on trays of the packed columns has not been studied as far as we are concerned. The present work aims for a better understanding of the physics behind the foam formation along with its prevention or inhibition, depending on the packing shape. Possible analytical and numerical solutions for laminar fully-developed flows through random or structured packings under the effect of gravity when the packings are located inside packed columns are investigated. As a starting point, a zig-zag geometry with an internal angle 2α is chosen. We propose an analytical expression that describes both the fluid behaviour through the chosen geometry and the shape of the interface generated between the liquid and the gas. Relevant parameters such as surface tension and contact angle are considered in the analysis.

Introduction

Random and structured column-packings (Billet and Schultes, 1999 and Brinkmann et al., 2011) provide effective transport of material and thermal energy between a gas and a liquid, for example in extraction, absorption, distillation, and rectification columns. Due to their special structure and arrangement, the packings try to create an interface as large as possible between liquid and gas. While the gas flows from the bottom of the column to the top, the liquid flows in the opposite direction as a trickle film along the surface of the packings. The laminar or turbulent impulse transport between the phases determines the surface behaviour. The packings have the potential to generate primary foams (Senger and Wozny, 2011), but they are also able to modify them by partial destruction through secondary foam formation.

[*] Corresponding author. E-mail: lidia.almazan@fau.de

GALA e.V., Karlsruhe, Germany, ISBN 978-3-9816764-6-4

According to Kister (2003), the formation of undesired foams occupies the place 11 out of 31 of the causes of column malfunctions. Products with undesired foam formation during their processing are found in food industry, for example soups, sugar, milk, juices, beer and spirits. In order to maintain the purity of the food, beverages and also fine chemicals the present work disregards from any use of chemical anti-foaming agents, therefore it focuses on the physical based management of the undesired foam.

For the physical foam management, the dynamic net foam balance (DNSB for its acronym in German)

$$\mathrm{DNSB} = \sum \text{Foam formation effect} - \sum |\text{Foam destruction effect}| \,,$$

plays an important role. Only negative values of this balance in stationary column operation prevent the formation of disturbing foam. As a consequence a question about the material, the process-technical boundary conditions and the area of existence of the foam arises. For an efficient foam management, we define the Deborah number (De) as

$$\mathrm{De} = \frac{\text{characteristic process time}}{\text{characteristic existence time}} \,,$$

which is the ratio of the characteristic process time and the existence time of the foam. The physical values defined above are expected to ensure negative values of DNSB and high values of De at any time of the process.

Column-packings exist as structured or random (Mackowiak, 2003). Structured packings consist predominantly of thin, structured and perforated metal plates or wire nets, which form a packed composite element. The packings create flow channels with a large specific exchange area for mass transfer. These packings completely fill the inner surface perpendicular to the column axis. On the other side, random packings are smaller structures randomly distributed in a tray inside the packing-column. The flow channels have orientations that usually deviate from the inner axis of the column. In addition to the large values of specific exchange area, good wettability and low flow resistance are also desired characteristics from the packings.

Wei et al. (2017) showed how in open-channel flows the free surface can trap an air bubble inside the liquid flow due to the interface deformation. This means that if many bubbles are trapped into the liquid, foam can be formed. This is directly related to the waves or flow structures that appear on the free surface of falling liquid flows, as shown by Dietze et al. (2014).

The present work is based on the hypothesis that depending on the geometry of the packages, there might be interface domains or free surfaces where no air entrainment into the liquid flow occurs, therefore proper geometries has to be found. For this purpose, an analytical and numerical treatment of the behaviour of a fluid flow in a chosen geometry is here presented, taking into account the liquid-gas free surface. This latter requires that different fluid quantities such as surface tension or contact angle have to be considered for the analysis.

Physical model

The starting point of the analysis is the characterization of the fluid flowing through the packages. The characterization is conducted by solving the Navier-Stokes equations (Spurk and Aksel, 2008) that describe mathematically the behaviour of the fluids along with the mass conservation equation,

GALA e.V., Karlsruhe, Germany, ISBN 978-3-9816764-6-4

$$\rho\left(\frac{\partial\vec{u}}{\partial t}+\vec{u}\cdot\nabla\vec{u}\right)=-\nabla p+\mu\nabla^2\vec{u}+\vec{F},$$
$$\nabla\cdot\vec{u}=0. \tag{1}$$

Here ρ is the density of the fluid, p is the hydrostatic pressure, μ is the dynamic viscosity, $\vec{u}$ is the velocity field and $\vec{F}$ represents any external force applied to the fluid.

The chosen geometry in the present work consists of an open channel with the walls forming an internal angle 2α in the $r\theta$-plane as it is shown in Fig. 1. For convenience cylindrical coordinates are chosen, while the walls are vertically disposed in the z-direction as depicted in Fig. 1a. Inside the packed columns, the liquid flows from top to bottom, while the gas is moving from the bottom to the top, with the gravity pointing downwards. The height of the triangular channel is defined by H, and the distance between the centre of the polar coordinates and the free surface is defined as a function of the angle θ as $h(\theta)$, see Fig. 1b. The contact angle γ is also represented in Fig. 1b and is the angle where the liquid-gas interface meets the solid surface. This angle depends on the wall material and the fluids themselves.

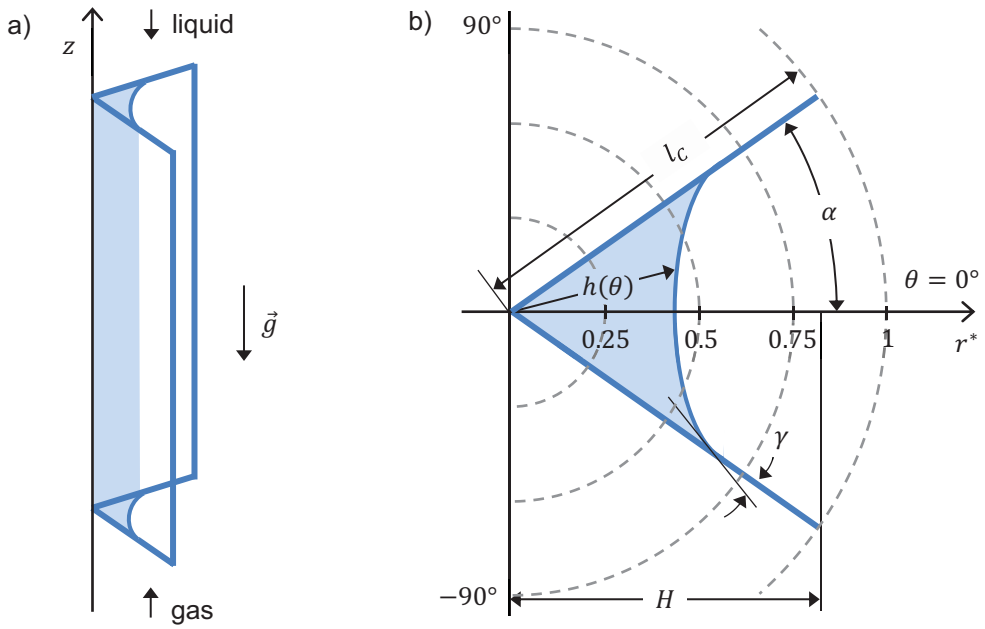

Fig. 1: Schematic of the chosen geometry of the open channel with two vertical walls forming an internal angle 2α, height H, interface $h(\theta)$, characteristic length l_C and contact angle γ. a) side view, b) top view.

Due to the complexity of the problem, the following assumptions are taken in order to analytically solve Eq. 1: the fluid is assumed Newtonian, while the flow is considered stationary, laminar and fully developed in cylindrical coordinates. Gravity as the unique external force is pointing downwards in z-direction. The cylindrical coordinates are preferred due to the symmetry of the chosen geometry. All the assumptions simplify the Navier-Stokes equations (Eq. 1) into one equation, given in dimensionless form by

$$\frac{\partial^2 u^*}{\partial r^{*2}}+\frac{1}{r^*}\frac{\partial u^*}{\partial r^*}+\frac{1}{r^{*2}}\frac{\partial^2 u^*}{\partial\theta^2}=\frac{\mathrm{Re}}{\mathrm{Fr}}, \tag{2}$$

GALA e.V., Karlsruhe, Germany, ISBN 978-3-9816764-6-4

where superscripts represent dimensionless quantities, Re is the Reynolds number, that describes the relative magnitudes of inertial and viscous forces in the system given by $\mathrm{Re} = \rho u_C l_C/\mu$, and Fr is the Froude number, representing the ratio of inertial and gravity forces, $\mathrm{Fr} = u_C^2/g l_C$. In the dimensionless numbers, u_C and l_C are the characteristic velocity and length respectively, $u^* = u/u_C$ and $r^* = r/l_C$, with the characteristic length defined as $l_C \equiv H\cos\alpha$, which is the width of the wall, as it is shown in Fig. 1b.

An analytical solution of the Eq. 2 requires proper boundary conditions. No-slip boundary conditions are considered for the walls, where the liquid in contact with the wall takes its velocity, which in this case is zero. The mathematical method used to solve Eq. 2 is separation of variables, which results are shown in the next section.

Results

The complexity of the free surface makes the problem difficult to handle. The no-slip boundary conditions were imposed on the walls, where $\theta = \pm\alpha$. Additionally, the velocity is assumed finite everywhere and in particular at $r^* = 0$. Furthermore, the problem is considered symmetric about the line at $\theta = 0$. The solution of the Eq. 2 in dimensionless form is given by

$$u^*(r^*,\theta) = \frac{1}{4}\frac{\mathrm{Re}}{\mathrm{Fr}}\left[r^{*2}\left(1-\frac{\cos(2\theta)}{\cos(2\alpha)}\right) - \sum_n C_n r^{*\frac{(2n-1)\pi}{2\alpha}}\cos\left(\frac{(2n-1)\pi\theta}{2\alpha}\right)\right], \tag{3}$$

where the angle $\theta \in [-\alpha, \alpha]$, n are integers with values $n \geq 1$ and C_n are coefficients which have to be found when the boundary condition of the free surface is implemented. The Eq. 3 provides a general expression for the velocity field for any internal angle 2α independently of the characteristic of the third boundary.

Firstly, an ideal flat free surface is assumed. For liquid-gas systems with a large density difference (e.g. $\rho_{water} = 1000\,kg/m^3 \gg \rho_{air} = 1.18\,kg/m^3$) the momentum exchange at the interface is significantly low and can be neglected. Mathematically it is given as

$$\left.\frac{\partial u^*}{\partial \vec{n}}\right|_{\Omega} = 0, \tag{4}$$

where $\vec{n}$ is a normal vector to the interface and Ω defines the interface. Assuming the free surface as flat, $\vec{n}$ is the same along the entire interface Ω, pointing in x-direction.

The results for the flow field are presented in Fig. 2 for an internal angle $2\alpha = 60°$, and the relation $\mathrm{Re}/\mathrm{Fr} = 1$. It can be seen that the maximum velocity is located symmetrically at $y = 0$ at the free surface, while the velocity is 0 at the walls. In Fig. 2 the boundary at maximum x^* represents the flat free surface.

In the second part of the analysis, the surface tension and the contact angle are introduced into the boundary conditions for a more realistic situation. The normal stress at the free surface must be balanced by the curvature pressure associated with the surface tension as

$$\vec{n}^T \cdot \vec{\vec{T}}^* \cdot \vec{n} = \frac{1}{\mathrm{We}}\left(\vec{\nabla}^* \cdot \vec{n}\right), \tag{5}$$

where We is the Weber number, which relates the fluid inertia and the surface tension, $\mathrm{We} = \rho u_C^2 l_C/\sigma$, and $\vec{\vec{T}}^*$ is the dimensionless stress tensor, defined for a Newtonian fluid (Spurk and Aksel, 2008) as

GALA e.V., Karlsruhe, Germany, ISBN 978-3-9816764-6-4

$$\vec{\vec{T}}^* = -p^* \mathrm{I}_3 + \frac{1}{\mathrm{Re}}\left[\vec{\nabla}^* \vec{u}^* + \left(\vec{\nabla}^* \vec{u}^*\right)^T\right], \tag{6}$$

where I_3 is the identity matrix and p^* is the dimensionless hydrostatic pressure with $p^* = p/u_C^2 \rho$. The contact angle γ is a geometrical condition that depends on the material of both the wall and fluids (liquid and gas). Therefore, this condition applies only where the fluid is in contact with the wall $\theta = \pm\alpha$, and is defined as,

$$\vec{n} \cdot \vec{n}_S = \cos\gamma, \tag{7}$$

where $\vec{n}_S$ is the normal vector to the wall.

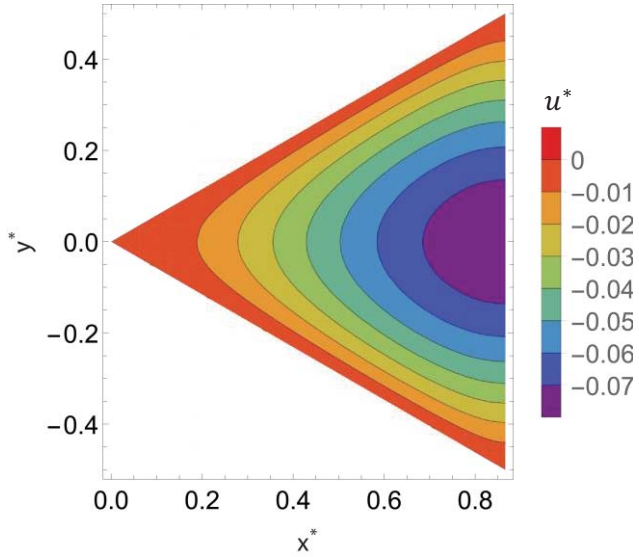

Fig. 2: Velocity flow field for an internal angle of $2\alpha = 60°$ and $\mathrm{Re}/\mathrm{Fr} = 1$, assuming an ideal flat free surface at maximum x^*.

The interface is defined as $r^* = h(\theta)$ in cylindrical coordinates, with the functional $f(r^*, \theta) = r - h(\theta)$ that necessarily vanishes on the surface. The normal to the surface is described by

$$\vec{n} = \frac{\vec{\nabla} f}{\left|\vec{\nabla} f\right|} = \frac{r^* \hat{r} - h'(\theta)\hat{\theta}}{\sqrt{r^{*2} + h'(\theta)^2}}, \tag{8}$$

where $h'(\theta) = dh(\theta)/d\theta$.

Substituting Eqs. 3, 6 and 7 into Eq. 5, the corresponding PDE for the pressure is obtained

$$p^* = \frac{1}{\mathrm{We}} \frac{h(\theta)^2 + 2h'(\theta)^2 - h''(\theta)h(\theta)}{(h(\theta)^2 + h'(\theta)^2)^{3/2}}. \tag{9}$$

An analytical solution of Eq. 9 is extremely complex, therefore some assumptions are again required to simplify the equation. It is assumed that the curvature of the interface is small, i.e. $h'(\theta)^2 \ll 1$, and also that $h(\theta) \lesssim 1$, this allows to linearize the Eq. 9 into the form,

$$p^* \mathrm{We} = 1 - h''(\theta). \tag{10}$$

Applying the boundary condition defined in Eq. 7, the solution of Eq. 10 for the interface taking into account the contact angle γ and the surface tension σ is given by

GALA e.V., Karlsruhe, Germany, ISBN 978-3-9816764-6-4

$$h(\theta) = (p^*\mathrm{We} - 1)\frac{\alpha^2 - \theta^2}{2} + \sqrt{(p^*\mathrm{We} - 1)^2\alpha^2 \tan(\gamma)^2}. \tag{11}$$

Equation 11 is a second order polynomial with dependence on the angle θ; the other terms are constant for each situation. In Fig. 3 the solution for the interface for contact angles $\gamma = 40°, 50°, 60°$ and $70°$ is presented. For the analysis $p^*\mathrm{We} = 0.8\cos\alpha$ and $2\alpha = 60°$. The results shown in Fig. 3 depend on the variables γ, α and $p^*\mathrm{We}$ which are related with the geometry size, the hydrostatic pressure, the material of the walls and the liquid properties.

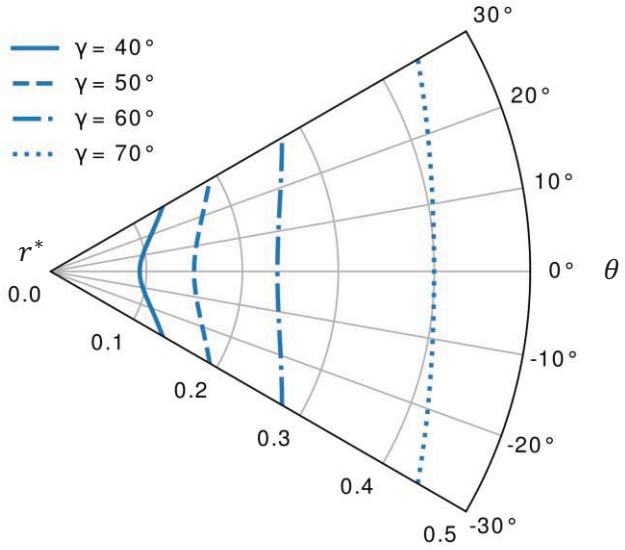

Fig. 3: Plot of the interface for different contact angles $\gamma = 40°, 50°, 60°$ and $70°$ with $p^*\mathrm{We} = 0.8\cos\alpha$ and $2\alpha = 60°$.

Figure 4 depicts the results for different values of the term $p^*\mathrm{We}$ for a given inner angle $2\alpha = 60°$ and the contact angle $\gamma = 60°$. The results show the change in the curvature of the interface from concave to convex as the pressure increases.

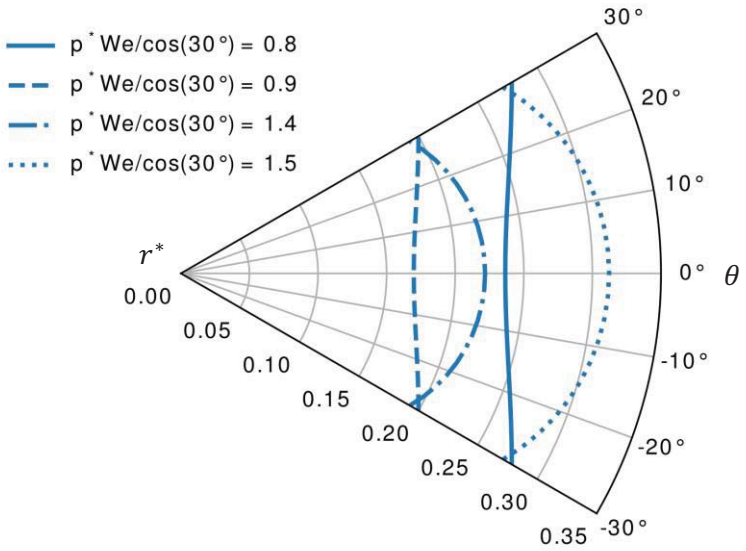

Fig. 4: Plot of the interface for different $p^*\mathrm{We}/\cos\alpha = 0.8, 0.9, 1.4$ and 1.5, with the contact angle $\gamma = 60°$ and $2\alpha = 60°$.

GALA e.V., Karlsruhe, Germany, ISBN 978-3-9816764-6-4

Once the function for the interface is obtained, the coefficients C_n in Eq. 3 can be calculated for the velocity field, applying the boundary condition Eq. 4 and computing the normal to the $h(\theta)$. Equation 4 is then transformed as

$$\frac{1}{\sqrt{r^{*2}+h'(\theta)^2}}\left(r^*\frac{\partial u^*}{\partial r^*}-\frac{h'(\theta)}{r^*}\frac{\partial u^*}{\partial \theta}\right)\Bigg|_{\mathrm{r}^*=h(\theta)}=0. \tag{12}$$

Substituing the Eq. 12 into Eq. 3, the corresponding coefficients C_n are obtained. The results in terms of the velocity field for two different contact angle $\gamma = 50°$ and $\gamma = 60°$ are shown in Fig. 5a and Fig. 5b, respectively. For the analysis $p^*\mathrm{We} = 0.8\cos\alpha$, $2\alpha = 60°$ and $\mathrm{Re/Fr} = 1$.

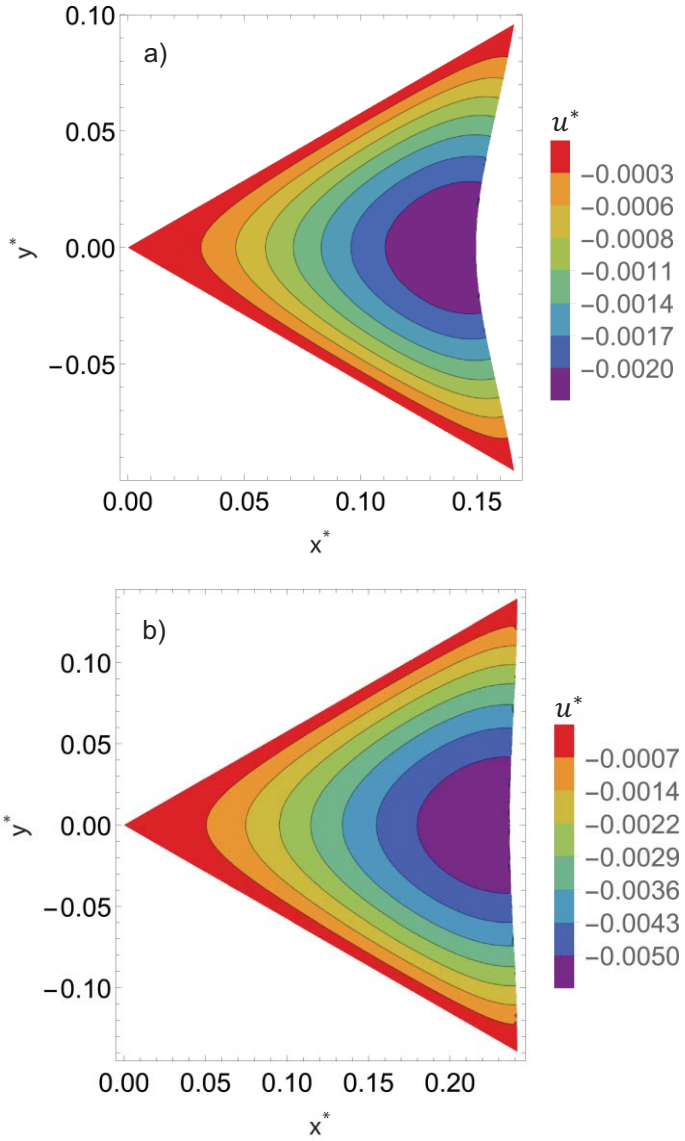

Fig. 5: Velocity flow field map for an internal angle $2\alpha = 60°$ and $\mathrm{Re/Fr} = 1$, considering two different contact angles a) $\gamma = 50°$ b) $\gamma = 60°$ fixing $p^*We = 0.8\cos\alpha$.

The results exhibit similar velocity distribution as those obtained with a flat free surface, with slight influence of the interface form. However, the maximum distance x^* where the liquid interface is located is smaller than the showed in Fig. 2. This is due to the fact that the maximum x^* showed in Fig. 2 contains a singularity on the corners, and therefore the width of the wall is not imposed as a condition when the interface function $h(\theta)$ is defined. Which also means that the volume flow is not preserved, but should be taken into account in the future.

GALA e.V., Karlsruhe, Germany, ISBN 978-3-9816764-6-4

Summary and Outlook

The present work provides a general solution for the velocity field of a flow in an open vertical channel. The solution is independent of the treatment of the free surface. Two different approximations of the liquid-gas interface were studied. The first case shows a solution of an idealized flat free surface, which physical contact angle corresponds to $60°$, for an inner angle $2\alpha = 60°$.

The second case assumes a more realistic interface, taking into account the properties of the fluids as well as the hydrostatic pressure. For the solution, it was assumed that the curvature of the interface is small, allowing to find an analytical expression for the interface by means of the normal stress balance. The obtained general expression is valid for any internal angle 2α and any contact angle.

The results shown in this work presents a baseline for the description of fluid behaviour in a geometry of two plates with an internal angle 2α. Further work comprises the accomplishment of experimental studies in order to collect physical data for comparison and validation. In a final stage, the stability of the liquid-gas interface will be studied to find possible non-existence domain for bubble formation.

Acknowledgements

The authors gratefully acknowledge the support given by the German Science Foundation (DFG) with the project number 408062554 in the frame of the DFG/AiF-Cluster (CV) 6 “Physikalisches Management störender Schäume”.

References

Billet, R., Schultes, M., 1999: “Prediction of Mass Transfer Columns with Dumped and Arranged Packings”, Chem. Eng. Res. Des., 77(6), pp. 498-504

Brinkmann, U., Kaibel, B., Jödecke, M., Mackowiak, J., Kenig, E. Y., 2011: “Beschreibung der Fluiddynamik von Anstaupackungen”, Chem. Ing. Tech., 84(1-2), pp. 36-45

Dietze, G., Rohlfs, W., Nährich, K., Kneer, R., Scheid, B., 2014: “Three-dimensional flow structures in laminar falling liquid films”, J. Fluid Mech., 743, 75-123

Kister, H. Z., 2003: “What Caused Tower Malfunctions in the Last 50 Years?”, Chem. Eng. Res. Des., 81(1), pp. 5-26

Mackowiak, J., 2003: “Fluiddynamik von Füllkörpern und Packungen”, Springer-Verlag Berlin Heidelberg

Senger, G., Wozny, G., 2011: “Experimentelle Untersuchung von Schaum in Packungskolonnen”, Chem. Ing. Tech., 83(4), pp. 503-510

Sparrow, E. M., 1962: “Laminar flow in isosceles triangular ducts”, AIChE Journal, 8(5), pp. 599-604

Spurk, J.H., Aksel, N., 2008: “Fluid Mechanics”, Springer-Verlag Berlin Heidelberg

Wei, W., Xu, W., Deng, J., Tian, Z., Zhang, F., 2017: “Free-surface air entrainment in open-channel flows”, Sci. China Technol. Sci., 60(6), pp. 893-901

GALA e.V., Karlsruhe, Germany, ISBN 978-3-9816764-6-4